Electron beam water calorimetry measurements to obtain beam quality conversion factors

Muir, Bryan R.; Cojocaru, Claudiu D.; McEwen, Malcolm R.; Ross, Carl K.

Publisher's version / Version de l'éditeur:
https://doi.org/10.1002/mp.12463
Medical Physics, 44, 10, 2017-08-08

Electron beam water calorimetry measurements to obtain beam quality conversion factors

B.R. Muir[1], C.D. Cojocaru, M.R. McEwen and C.K. Ross

Measurement Science and Standards, National Research Council of Canada,
Ottawa, ON, K1A 0R6, Canada
[1]Bryan.Muir@nrc-cnrc.gc.ca

Last edited May 1, 2017

Abstract

Purpose: To provide results of water calorimetry and ion chamber measurements in high-energy electron beams carried out at the National Research Council Canada (NRC). There are three main aspects to this work: 1) investigation of the behavior of ionization chambers in electron beams of different energy with focus on long-term stability, 2) water calorimetry measurements to determine absorbed dose to water in high-energy beams for direct calibration of ion chambers, and 3) using measurements of chamber response relative to reference ion chambers, determination of beam quality conversion factors, k_Q, for several ion chamber types.

Methods: Measurements are made in electron beams with energy between 8 MeV and 22 MeV from the NRC Elekta *Precise* clinical linear accelerator. Ion chamber measurements are made as a function of depth for cylindrical and plane-parallel ion chambers over a period of five years to investigate the stability of ion chamber response and for indirect calibration. Water calorimetry measurements are made in 18 MeV and 22 MeV beams. An insulated enclosure with fine temperature control is used to maintain a constant temperature (drifts less than 0.1 mK/min) of the calorimeter phantom at 4 °C to minimize effects from convection. Two vessels of different designs are used with calibrated thermistor probes to measure radiation induced temperature rise. The vessels are filled with high-purity water and saturated with H_2 or N_2 gas to minimize the effect of radiochemical reactions on the measured temperature rise. A set of secondary standard ion chambers are calibrated directly against the calorimeter. Finally, several other ion chambers are calibrated in the NRC ^{60}Co reference field and then cross-calibrated against the secondary standard chambers in electron beams to realize k_Q factors.

Results: The long-term stability of the cylindrical ion chambers in electron beams is better (always < 0.15 %) than plane-parallel chambers (0.2-0.4 %). Calorimetry measurements made at 22 MeV with two different vessel geometries are consistent within 0.2 % after correction for the vessel perturbation. Measurements of absorbed dose calibration coefficients for the same secondary standard chamber separated in time by 10 years are within 0.2 %. Drifts in linac output that would affect the transfer of the standard are mitigated to the 0.1 % level by performing daily ion chamber normalization measurements. Calibration coefficients for secondary standard ion chambers can be achieved with uncertainty less than 0.4 % (k=1) in high-energy electron beams. The additional uncertainty in deriving calibration coefficients for well-behaved chambers indirectly against the secondary standard reference chambers is negligible. The k_Q factors measured here differ by up to 1.3 % compared to those in TG-51, an important change for reference dosimetry measurements.

Conclusions: The measurements made here of k_Q factors for eight plane-parallel and six cylindrical ion chambers will impact future updates of reference dosimetry protocols by providing some of the highest quality measurements of this crucial dosimetric parameter.

This table of contents is for drafting and review purposes only.

Contents

I. Introduction

I.A. Electron beam clinical reference dosimetry

Linear accelerators for external beam therapy are calibrated in terms of absorbed dose to water using ion chambers with absorbed dose calibration coefficients traceable to national standards. The absorbed dose to water, D_{w}, at the reference point in the absence of the detector is determined with

$$D_{\mathrm{w}} = M N^{Q}_{\mathrm{D,w}}, \tag{1}$$

where $N^{Q}_{\mathrm{D,w}}$ is the ion chamber absorbed dose calibration coefficient in a beam of quality Q, determined for the user chamber at a primary standards dosimetry laboratory (PSDL), an accredited dosimetry calibration laboratory (ADCL) or a secondary standards dosimetry laboratory (SSDL) and M is the ion chamber reading measured under reference conditions in water. Absorbed dose to water calibration protocols such as the AAPM's TG-51[1,2] and the IAEA's TRS-398[3] specify the procedures to be followed for beam calibration.

It is normally not possible to obtain $N^{Q}_{\mathrm{D,w}}$ coefficients for ion chambers in the accelerator beam corresponding to the beam of quality Q used for clinical treatments. For this reason, calibration laboratories normally calibrate ion chambers in a ^{60}Co reference field to provide the user with $N^{\mathrm{Co}}_{\mathrm{D,w}}$. Equation 1 then becomes

$$D_{\mathrm{w}} = M k_{Q} N^{\mathrm{Co}}_{\mathrm{D,w}}, \tag{2}$$

which requires the beam quality conversion factor, k_Q, to convert the reading of the ion chamber measured in the clinical beam with the ^{60}Co calibration coefficient to the absorbed dose to water.

If one has a mechanism to establish absorbed dose to water (*e.g.* , using water calorimetry measurements) and measures the fully corrected ion chamber reading to obtain $N_{\mathrm{D,w}}$ coefficients in a linac beam of quality Q and a ^{60}Co reference field, equations 1 and 2 can be combined to realize measured k_Q factors through

$$k_{Q} = \frac{N^{Q}_{\mathrm{D,w}}}{N^{\mathrm{Co}}_{\mathrm{D,w}}}. \tag{3}$$

The TG-51 protocol factors k_Q for electron beams as

$$k_{Q} = P_{\mathrm{gr}} k_{R_{50}} = P_{\mathrm{gr}} k_{\mathrm{ecal}} k'_{R_{50}}, \tag{4}$$

where P_{gr} is the gradient correction, measured in the beam of interest, and $k_{R_{50}}$ is the component of k_Q independent of gradient effects. The factor $k_{R_{50}}$ is further factored into k_{ecal}, the photon-electron conversion factor, which is $k_{R_{50}}$ for a high-energy electron beam of quality Q_{ecal}, and $k'_{R_{50}}$, the electron quality conversion factor.

Calculations of $k_{R_{50}}$ for the TG-51 protocol used a semi-analytic approach via

$$k_{R_{50}} = \frac{\left[\left(\frac{\bar{L}}{\rho}\right)^{\text{water}}_{\text{air}} P_{\text{cel}} P_{\text{fl}} P_{\text{wall}}\right]^{Q}}{\left[\left(\frac{\bar{L}}{\rho}\right)^{\text{water}}_{\text{air}} P_{\text{cel}} P_{\text{repl}} P_{\text{wall}}\right]^{\text{Co}}}, \tag{5}$$

where $\left(\frac{\bar{L}}{\rho}\right)^{\text{water}}_{\text{air}}$ is the electronic water to air mass stopping power ratio, $P_{\text{repl}} = P_{\text{gr}} P_{\text{fl}}$ corrects for the introduction of an air cavity, P_{cel} corrects for the lack of air-equivalence of the chamber's central electrode and P_{wall} corrects for the lack of water-equivalence of the chamber wall. The possibility of measured k_Q factors removes the need for the semi-analytic approach of equation 5, which contains a number of assumptions for both cylindrical and parallel-plate chambers that are now disputed, and should result in a much lower overall uncertainty. Therefore, there is motivation for an investigation to accurately determine electron beam quality conversion factors for both chamber types.

I.B. Water calorimetry

The most common technique used to realize absorbed dose to water for megavoltage photon and electron beams in a primary way is calorimetry. Calorimeters developed by National Measurement Institutes (NMIs) worldwide have focused on two low-Z materials relevant to the dosimetry of radiation therapy beams, water and graphite. Each material offers certain advantages for the measurement of dose and DuSautoy,[4] Seuntjens and Duane[5] and McEwen[6] provide comprehensive reviews of calorimetry development and operation of both water and graphite calorimeters. Much of the research to date has, perhaps not surprisingly, focused on calorimetry for ^{60}Co and megavoltage photon beams, although investigations have been carried out for ^{192}Ir HDR brachytherapy[7,8] and kV x-ray beams[9,10]. Except for a small number of research groups, research into calorimetry for high-energy electron beams has been very limited. McEwen and DuSautoy reviewed the status of primary dosimetry standards for such radiation beams in 2009[11] and Renaud *et al.*[12] provide an update on the results presented there for the McGill University water calorimeter. The Ionizing Radiation

Standards group at the NRC has been active in calorimetric standards for electron beams for more than a decade (initial work was presented by McEwen and Ross[13]) and the results presented here cover measurements over that entire period.

The principle behind absorbed dose determination using calorimetry measurements is relatively straightforward. The absorbed dose to medium, D_{m}, is measured using

$$D_{\mathrm{m}} = c_{\mathrm{p}} \Delta T, \tag{6}$$

where c_{p} is the specific heat capacity of the medium at constant pressure and ΔT is the radiation induced temperature rise. The specific heat capacity of water is well known.[14] By only requiring measurements of temperature rise one relies only on primary standards for temperature and the measurement is therefore independent of any other measurements in radiation beams.

In practice, water calorimetry measurements are difficult to realize because of the very small increase in temperature from radiation (0.5 mK for a dose of 2 Gy), requiring low uncertainty in the temperature measurement in order to be useful. Various corrections are also required. There are additional difficulties introduced when performing measurements in electron beams (*e.g.* steep dose distributions). The procedure employed for temperature measurement using the NRC calorimeter and corrections required is reviewed in section II..

I.C. Ion chamber calibration

It is impractical to perform routine water calorimetry measurements to calibrate chambers directly. Therefore, absorbed dose to water calibration coefficients are normally obtained by calibrating ion chamber readings indirectly against secondary standard reference chambers. The behavior of these reference chambers is fully characterized and are known to be stable at the 0.1 % level over periods of up to 15 years[15]. If readings are obtained from any ion chamber, M_{ch}, and from a reference ion chamber, M_{ref}, which has been calibrated directly against the primary standard calorimeter to obtain $N_{\mathrm{D,w,ref}}$ in a given beam, the absorbed dose to water calibration coefficient for the chamber to be calibrated, $N_{\mathrm{D,w,ch}}$, can be obtained through equation 1 with

$$N_{\mathrm{D,w,ch}} = \frac{M_{\mathrm{ref}}}{M_{\mathrm{ch}}} N_{\mathrm{D,w,ref}}. \tag{7}$$

We previously reviewed the accuracy of this indirect method of calibration for MV photon beams[15]. In fact, the only available electron beam ion chamber calibration service, offered by the National Physical Laboratory (NPL) in the UK, is based on this method of calibration.[16]

II. Methods

II.A. Water calorimetry measurements

II.A.1. Measurement of temperature rise

The NRC primary standard water calorimeter has been described previously[17,18] and will be briefly discussed here. The steps to realize radiation induced temperature rise are:

1. Platinum resistance temperature detectors, RTDs, are calibrated to be traceable to the NRC primary standard for temperature. The output of the RTDs is measured with a digital multimeter. Readings are made as the temperature of the liquid (antifreeze and water mixture) is varied between -4 and 12 °C using a circulating chiller. These RTDs serve two purposes, calibration of the thermistor probes described in the next step and monitoring drifts in temperature in the calorimeter phantom before and after calorimeter runs.

2. Thermistor probes, built in house using negative temperature coefficient (NTC) glass thermistor beads (General Electric Thermometrics), are calibrated against the RTDs described in step 1 with the same set-up. Temperature is varied for these measurements between 0.5 and 7.5 °C to determine the relationship between thermistor resistance and temperature.

3. The 30×30×30 cm^3 calorimeter phantom is thermally isolated from the surrounding environment in a wooden enclosure with Styrofoam®insulation. The water in the calorimeter phantom is controlled at 4.00±0.03 °C to eliminate effects from convection[19]. Drifts in temperature are less than 0.1 mK/min before making measurements. Figure 1 shows a schematic of the NRC water calorimeter enclosure and set-up.

4. The thermistor probes are positioned 1 cm apart in the center of glass vessels that are filled with high purity water and saturated with either N_2 or H_2 gas to minimize effects from energy appearing as radiochemical reactions.[20,21] Two vessels are used in this work. A cylindrical flame-sealed glass vessel, which has produced consistent results over 17 years for photon beam measurements at NRC,[22] can be positioned with the thermistor probes at the reference depth in a 22 MeV electron beam. A plane-parallel glass vessel was designed

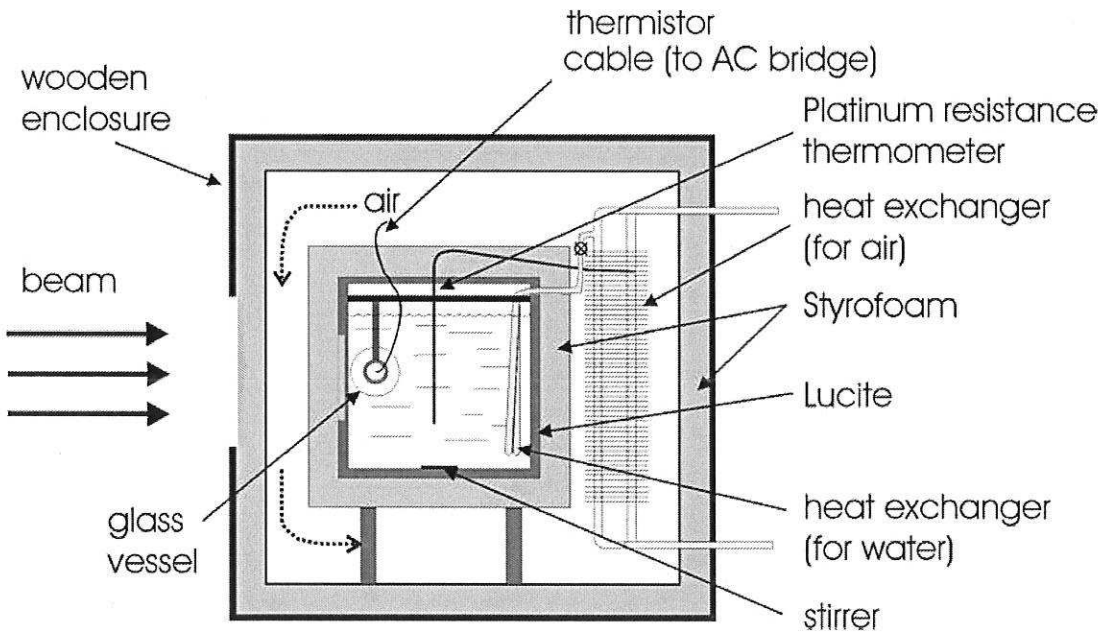

Figure 1: A schematic of the NRC water calorimeter enclosure and set-up.

specifically for measurements in electron beams and can be positioned with the thermistor probes at the reference depth ($d_{ref} = 0.6R_{50} - 0.1$ cm) in 18 MeV and 22 MeV beams. Figure 2 shows the vessels used for this work.

5. The change in resistance of the thermistors is measured using an AC bridge circuit as shown by McEwen and DuSautoy[11]. The voltage output of the bridge is measured with a Stanford Research Systems (SRS) SR830 DSP lock-in amplifier. The system is calibrated in terms of resistance vs voltage by measuring the change in voltage when the precision resistance decade box (Hochpräzisions-Widerstands-Dekade Typ 1422) changes the balancing resistor in the bridge circuit by one ohm ($\pm$ 0.05 %).

6. A typical calorimeter run consists of measuring the voltage in the bridge circuit for a period of 120 s before irradiation (pre-irradiation drift), followed by a 120 s irradiation and 120 s monitoring following irradiation (post-irradiation drift). Fits are then made to the pre- and post-irradiation drift to extrapolate to the voltage change at the midpoint of irradiation. Figure 3 shows an example of a typical calorimeter run showing bridge output voltage as a function of time.

7. Finally, the measured voltage change is converted through the calibration chain to temperature rise (voltage to resistance to temperature) and the corrections to the calorimeter reading discussed in the following section are applied.

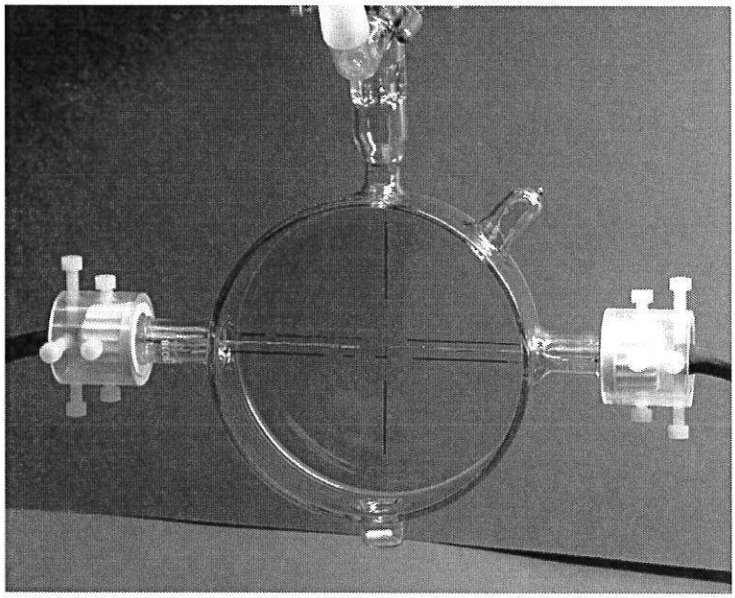

(a)

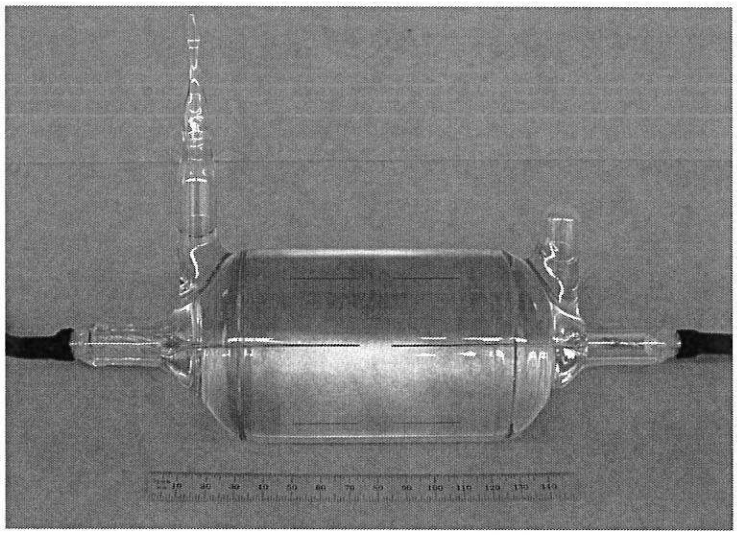

(b)

Figure 2: The vessels used in this work. Panel (a) shows the plane parallel vessel while panel (b) shows the sealed cylindrical vessel.

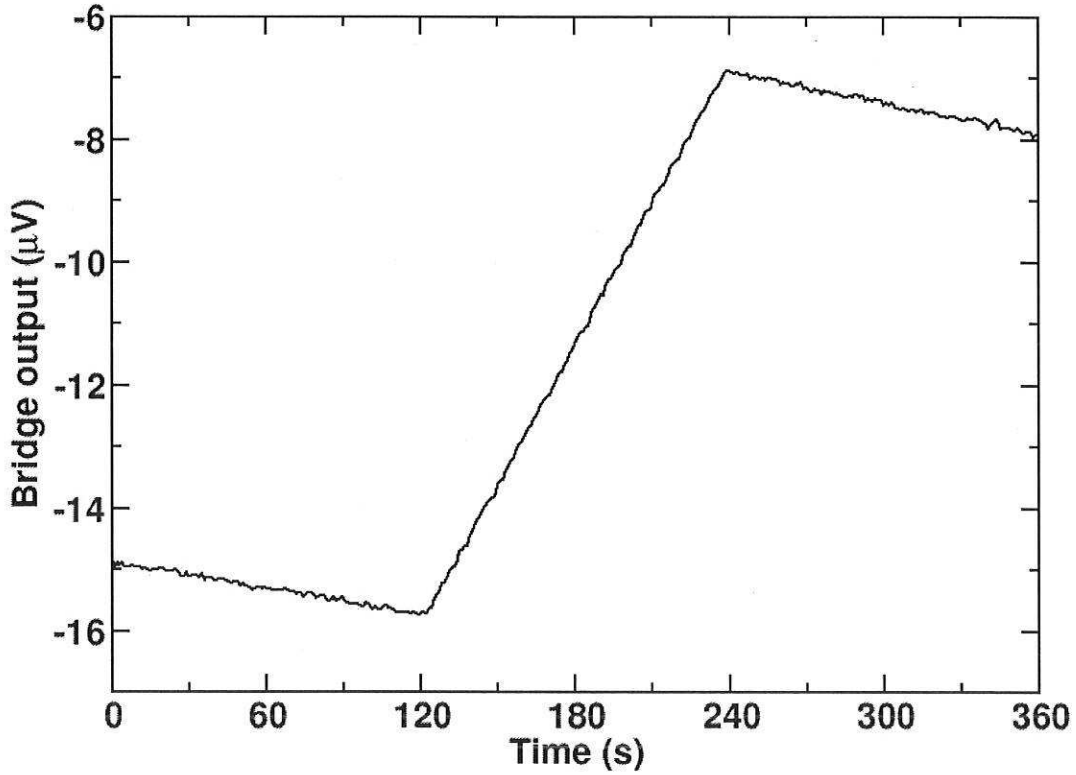

Figure 3: An example calorimeter trace.

II.A.2. Calorimeter corrections

As indicated in section I.B., there are several corrections required to perform accurate water calorimetry measurements, making equation 6 more complicated as

$$D_{\mathrm{w}} = c_{\mathrm{w}} \Delta T_{\mathrm{w}} k_{\mathrm{t}} k_{\mathrm{c}} k_{\nu} k_{\mathrm{p}} k_{\mathrm{dd}} k_{\rho} \frac{1}{1 - k_{\mathrm{HD}}}. \tag{8}$$

The various corrections to the measurement of temperature change are:

k_{t} corrects for any radiation-induced effects on thermistor response that persist after the beam is turned off. Measurements[23] show that the effect is negligible.

k_{c} corrects for effects from conductive heat transfer. This correction takes account of both the radial and axial dose distributions and also the increased heating effect of the glass wall of the calorimeter vessel. It is determined by solving the 2D heat transport equations using finite element analysis.

k_{ν} corrects for effects from convective heat transfer. This is assumed unity because the calorimeter is operated at 4 °C to mitigate these effects.[19]

k_p corrects for the perturbation from the introduction of the glass vessel and probes. The correction for the probes is assumed to be unity because they are so small (0.28 mm diameter) that they will not affect the measurement. The correction for the perturbation caused by the introduction of the glass vessel is measured using a diode detector with and without a dummy vessel for the cylindrical vessel design. For the plane-parallel vessel, the correction is determined by placing glass sheets in front and behind of the diode detector. This latter method is also compared to corrections determined using depth-dose curves and scaling the glass for water-equivalence.

k_{dd} corrects for non-uniformity of the radial dose profile at the point of measurement. This is determined using diode scans across the profile.

k_ρ corrects for the difference in density of water at 4 and 22 °C. This is determined through with physical data for water and the impact on the depth-dose curve.

k_{HD} corrects for the heat defect, the difference between absorbed energy from radiation and that which appears at heat. Since the high-purity water is saturated with N_2 or H_2 gas to minimize radiochemical reactions this correction is assumed to be negligible.[20,21]

II.A.3. Calorimeter set-up geometry

Two thermistor probes are positioned and aligned with cross-hairs at the center of the glass vessels. The probes are positioned horizontally about 1 cm apart in the center of the vessel. The precise depth of the probes within the plane-parallel vessel is determined using a travelling microscope with a dial gauge and correcting for the refractive index of glass.

The calorimeter phantom is positioned with a calibrated mechanical pointer at an SSD of 100 cm and aligned on the beam axis using cross-hairs at the center of the phantom on the front and back windows. The vessel with probes is aligned at the center of the phantom. The vessel is then positioned using a mechanical stand-off such that the probes are at the reference depth, accounting for the water-equivalent thickness of the calorimeter phantom window, the Styrofoam®insulation and the position of the probes within the vessel.

The geometry of the calorimeter enclosure does not allow the use of a standard electron applicator fitted to the NRC Elekta Precise linac, so the electron beam is collimated using a custom built 10×10 cm^2 applicator made from layers of lead and aluminium. This is mounted inside the calorimeter enclosure between the two layers of Styrofoam®shown in figure 1. The

collimator jaws are set to 16×16 cm^2. The reference depths for the 18 MeV and 22 MeV beams are taken as 4.20 cm and 5.26 cm using $d_{\text{ref}} = 0.6R_{50} - 0.1$ cm as recommended in dosimetry protocols[1,3] and using R_{50} measurements from depth-dose measurements obtained with diode detectors, verified using measurements with plane-parallel ion chambers.

II.A.4. Linac output monitoring

The size of the calorimeter enclosure means that it is not possible to have a side-by-side setup with the water calorimeter and ion chamber to be calibrated alternated in the linear accelerator beam. Some system is therefore required to transfer the dose rate measured by the water calorimeter to the in-water ion chamber measurements. We rely on the stability of the internal linac monitor chamber and transmission chamber to transfer the absorbed dose standard for ion chamber calibrations. To monitor the stability of these chambers, which track drifts in linac output, we use an NE2571 ion chamber mounted on the linac accessory plate in an aluminum holder such that the chamber can be positioned reproducably to better than 0.1 mm along the beam axis and ±0.25 mm radially. Figure 4 shows this set-up. One can also see the external transmission monitor chamber in this photograph. Measurements with the externally mounted NE2571 chamber are performed before calorimetry measurement begin for the day, between sets of calorimetry runs and at the end of a day of measurements and before/after in-water ionization chamber measurements. This approach was prototyped during water calorimeter measurements in linac photon beams and is current practice in the protocol of the BIPM key comparison BIPM.RI(I)-K6 "Measurement of absorbed dose to water for high-energy photon beams".[24]

II.B. Ion chamber measurements

II.B.1. Measurements for direct calibration

Ion chamber measurements are required to obtain absorbed dose calibration coefficients through equation 1 with dose to water known from calorimetry measurements. The fully corrected ion chamber reading, M, is determined from the raw chamber reading, M_{raw}, through

$$M = M_{\text{raw}} P_{\text{ion}} P_{\text{pol}} P_{\text{TP}} P_{\text{elec}} P_{\text{rp}} P_{\text{long}} \tag{9}$$

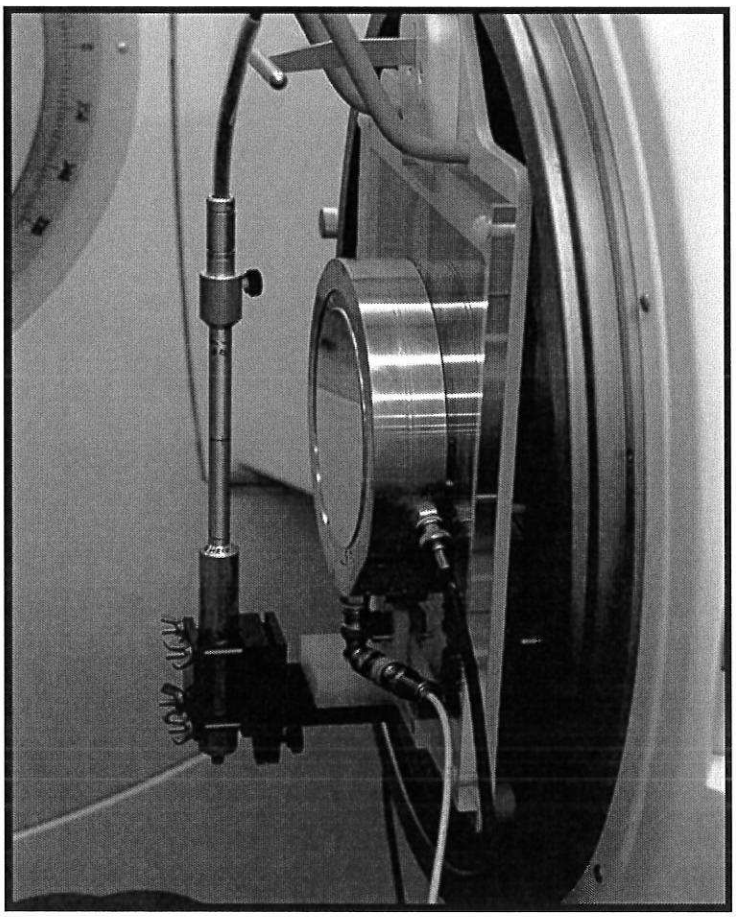

Figure 4: The NE2571 ion chamber mounted on the linac accessory plate for monitoring drifts in linac output over the course of measurements. This chamber is removed during actual measurements with the calorimeter or in-water ion chamber measurements. The external transmission chamber can also be seen mounted on the applicator plate.

where the corrections to the reading are the same as in the addendum to the TG-51 protocol[2] except for P_{long}, which corrects for the difference in irradiation time for chamber measurements and calorimetry measurements. Ion recombination corrections are determined with P_{ion} expressed as a function of D_{pp} from previous measurements. All other corrections are determined using the methods prescribed in the TG-51 protocol and addendum.

For measurements in 2006, one NE2571, one PTW Roos and one NACP-02 chamber were used for direct calibrations against the primary standard for absorbed dose. In 2016, measurements were repeated with the NE2571 chamber used in 2006 and were also made using an additional NE2571 chamber and a PTW30013 chamber. The irradiation geometry is

the same as for calorimetry measurements. Cylindrical chambers are positioned with the axis of their collecting volume aligned with and perpendicular to the beam axis. The cylindrical chambers' point of measurement is taken as the center of the chamber and positioned at the same reference depth as for calorimetry measurements. Plane-parallel chambers are positioned with their front face toward the beam. The chambers' front window is scaled for water-equivalence to determine the effective point of measurement.

II.B.2. Uncertainty budget

Table 1 provides an uncertainty budget for measurements of ion chamber calibration coefficients derived through direct calibration against the calorimeter. These uncertainties are estimated following the Guide to the Expression of Uncertainty in Measurements[25]. Component 3 is determined as the variation in the ratio of the NE2571 chamber mounted on the accessory plate to either the linac monitor chamber reading or the external transmission monitor compared to the first measurement of the day. Component 18 is derived from repeated ion chamber calibrations for well-behaved chambers discussed in section II.B.3.. Several components in table 1 for electron beams are correlated with the similar uncertainty budget for photon beams.

II.B.3. Depth-ionization measurements

Over the course of five years, repeated depth-ionization measurements have been made with several plane-parallel and cylindrical ion chambers in 8, 12 and 18 MeV electron beams according to the methods in our previous publication.[26] The purpose of these measurements is to investigate absorbed dose to water calibration coefficients derived relative to secondary standard ion chambers through equation 7 and monitor long-term stability of calibration coefficients. The accuracy of this method to derive ion chamber calibration coefficients using relative depth-ionization measurements was reviewed in that publication.

A brief review of this method is presented here and the reader is referred to our previous publication[26] for more details. The field size is defined with the typical clinical applicator to 10×10 cm^2. Two cylindrical ion chambers are mounted on the inside of the applicator such that they are not in the collimated beam at the phantom for monitoring linac drifts. Ion chambers are positioned along the beam axis using a precision mechanical stand-off to

Table 1: Uncertainty budget for determination of ion chamber calibration coefficients and beam quality conversion factors when chambers are calibrated directly against the primary standard calorimeter.

	Source and type of uncertainty	^{60}Co (%)	18 MeV (%)	22 MeV (%)
Type A				
1	Reproducibility ΔT/MU	0.08	0.14	0.18
2	Short term reproducibility M_{corr}/MU	0.02	0.01	0.02
3	Reproducibility linac monitors		0.08	0.08
Type B				
	Calorimeter related quantities			
4	$c_{w,p}$ (specific heat capacity)	< 0.005	< 0.005	< 0.005
5	Thermistor sensitivity	0.08	0.08	0.08
6	k_c (heat loss)	0.10	0.10	0.10
7	k_p (vessel perturbation)	0.05	0.10	0.10
8	k_{HD} (heat defect)	0.15	0.15	0.15
9	k_ρ (density of water)	0.02	0.02	0.02
10	k_{dd} (profile non-uniformity)	0.01	0.05	0.05
11	Positioning calorimeter, probes and vessel	0.13	0.12	0.12
	Chamber related quantities			
12	P_{rp}	0.03	0.05	0.05
13	P_{ion}	0.07	0.08	0.08
14	P_{pol}	0.01	0.03	0.03
15	P_{elec}	0.01	0.01	0.01
16	P_{long}		0.05	0.05
17	Positioning chamber	0.05	0.14	0.14
18	Ion chamber stability	0.05	0.06	0.06
	Combined uncertainty			
	$N_{D,w}$	0.27	0.35	0.37
	k_Q		0.30	0.32

define a reference location within the water phantom. Chambers are preirradiated with 1000 MU and then scanned through the phantom, pausing to collect charge for five seconds at each step. Scans are performed at each polarity to correct the readings for polarity effects. The readings are fully corrected using equation 9 although in this case P_{long} is not required. Finally, relative absorbed dose to water calibration coefficients are derived through equation 7 by comparing a given chamber reading to the reading of a reference class chamber calibrated directly against the water calorimeter.

Plane-parallel ion chambers investigated are (number of chambers of each type in parentheses):

PTW Roos (2),
PTW Markus (2),
PTW Advanced Markus (2),
Scanditronix NACP-02 (1),
IBA PPC-05 (2),
IBA PPC-40 (2),
Exradin A11 (1),
Exradin A10 (1).

Cylindrical ion chambers investigated are (number of chambers of each type in parentheses):
NE2571 (5),
IBA FC65-G (2),
PTW30013 (2),
Exradin A19 (1),
Exradin A18 (1),
Exradin A1SL (1).

III. Results

III.A. Measurement of absorbed dose

Figure 5 shows the calorimeter results obtained with the plane-parallel calorimeter vessel in 22 MeV. Each point on the plot represents a calorimeter run (see for example figure 3). Different sets of runs, typically 9-11, are shown with different symbols. The average standard uncertainty for a set of ten runs is 0.1 % when using the sealed cylindrical vessel, which is similar to results obtained in MV photon beams. The average standard uncertainty is slightly larger between 0.14-18 % when using the unsealed plane-parallel vessel. A set of runs is acquired over a period of a few hours before the temperature of the calorimeter phantom must be equilibrated. Between sets, measurements are made with an ion chamber mounted on the linac head as described in section II.A.4. to track drifts in linac output and transfer the absorbed dose standard to directly calibrate secondary standard ion chambers.

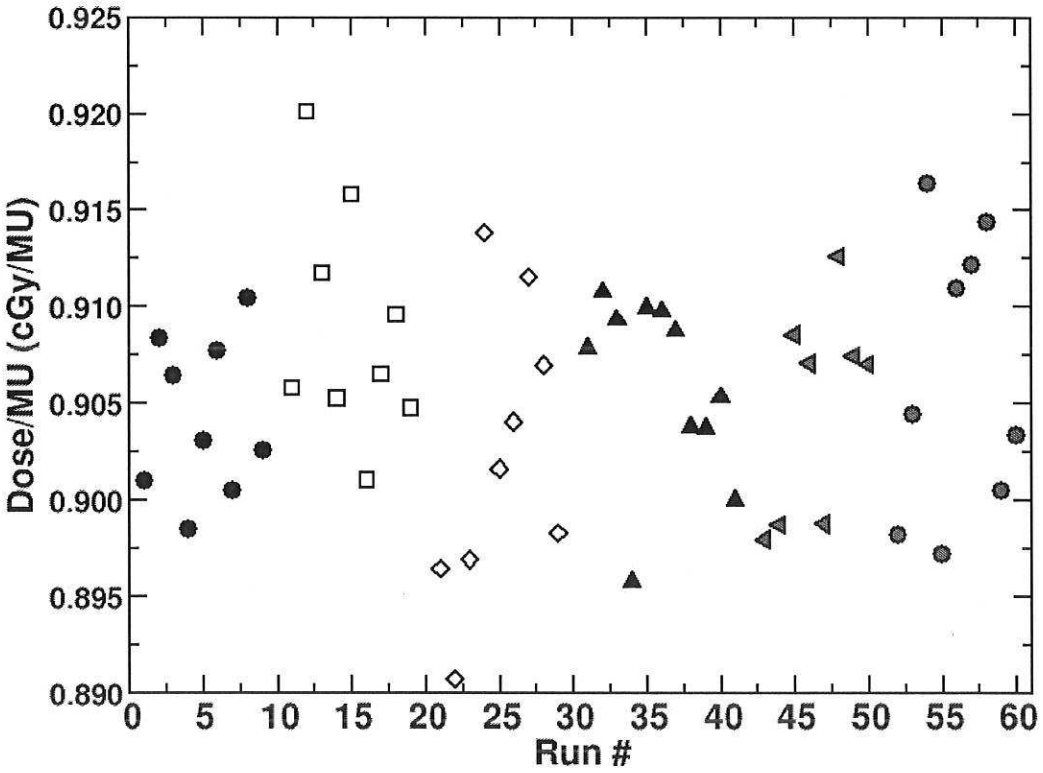

Figure 5: The results of the 22 MeV calorimeter runs using the plane-parallel calorimeter vessel. Different symbols represent one set of runs acquired over an approximately two hour period before reequilibrating the temperature of the calorimeter phantom.

III.B. Transfer of standard

As noted in section II.A.4. the dose measured by the calorimeter is transferred to the ion chamber to be calibrated via a Farmer-type chamber (NE2571) mounted on the linac accessory plate. This is not ideal, as the chamber must be removed for actual irradiation of the calorimeter or ionization chamber in-phantom, but the need for this monitor chamber in addition to the internal and external transmission monitors is demonstrated in figure 6 (a). The assumption is that the NE2571 chamber demonstrates the usual stability for such graphite-walled Farmer-type chambers (< 0.1 % variation per year) and this is combined with the positioning reproducibility noted in section II.A.4. to give a very precise measure of the beam output over the course of the calorimeter measurements (multiple weeks). If the transmission monitors were stable at the same level then one would expect a constant value for the

370 ratio $M_{\text{mon}}/M_{\text{NE2571}}$ (for a fixed electron energy). As can be seen in figure 6 (a), there is
371 a significant variation with time (up to 0.8 %) for both monitor chambers. There appears
372 to be some correlation for the two transmission chambers, which is perhaps to be expected
373 since they are of a similar open-to-atmosphere design. Figure 6 (b) shows that although the
374 transmission monitors are not stable enough from day-to-day, they have sufficient stability
375 to track the linac output over the course of a day. In figure 6 (b) each monitor reading is
376 normalized to the first NE2571 reading (setup as figure 4) each day and "Set index" refers to
377 a set of approximately 10 calorimeter irradiations (the day is not relevant for this analysis).
378 One can see now that the variations are much smaller, typically at the 0.1 % level. The
379 transmission chambers are therefore used for intra-day monitoring, the NE2571 chamber
380 mounted on the accessory plate is used for inter-day monitoring, and the combination allows
381 the accurate transfer of the dose measured by the calorimeter to the ionization chamber of
382 interest positioned in the water phantom at a separate time.

383 III.C. Direct calibration of secondary standard ion chambers

384 Table 2 provides absorbed dose to water coefficients, $N_{\text{D,w}}$, and beam quality conversion
385 factors, k_Q, for chambers determined through direct calibration against calorimetry mea-
386 surements. The values are obtained in 2006 and 2016. For the NE2571 chamber that
387 was calibrated at both times, the difference in $N_{\text{D,w}}$ obtained in 2006 and 2016 is 0.21 % for
388 22 MeV and 0.04 % in 18 MeV. Given that we know from independent testing of the NE2571
389 chamber in a Co beam that it has demonstrated stability of ± 0.1 % over two decades, this
390 level of repeatability is a measure of our ability to realise absorbed dose to water using the
391 primary standard water calorimeter. The difference between k_Q factors for the two NE2571
392 chambers is less than 0.1 %.

393 III.D. Beam quality conversion factors for several other chambers

394 Table 3 provides k_Q factors for several chambers by indirectly comparing chamber readings
395 to those from secondary standard ion chambers calibrated directly against the calorimeter
396 (see table 2) through equation 7. To obtain these k_Q factors, the average of the ratio of
397 chamber readings as a function of depth is taken close to the reference depth. Using the
398 uncertainty budget in table 2 of our previous publication[26] but replacing the uncertainty

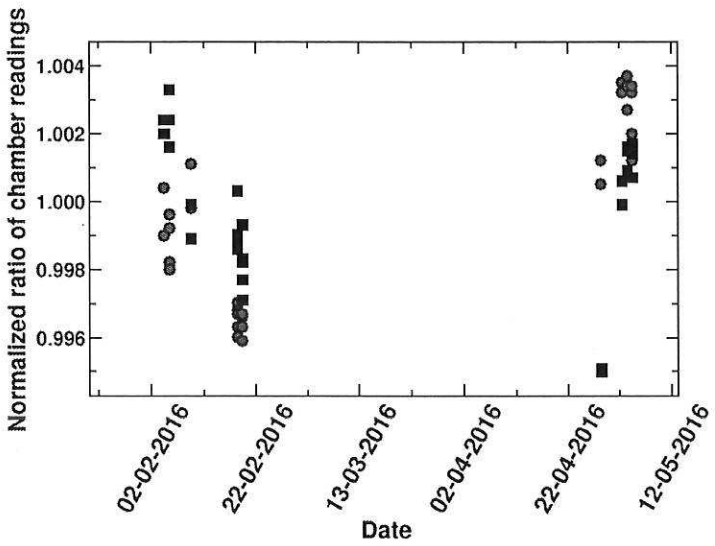

(a)

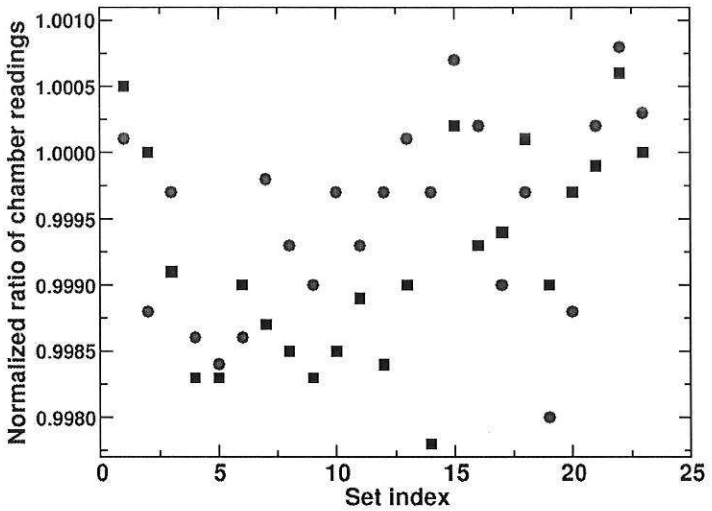

(b)

Figure 6: The ratio of readings from the NE2571 chamber mounted on the linac head between sets of calorimetry runs to that from either the internal linac monitor (circles) or the external transmission monitor (squares) that would affect the accuracy of the transfer of the absorbed dose standard to calibrate ion chambers. Panel (a) shows the results as a function of data obtained in 22 MeV during 2016, normalized to the mean of all readings while panel (b) shows the results as a function of set index normalized to the first measurement of the day.

Table 2: Absorbed dose to water calibration coefficients and beam quality conversion factors obtained through direct calibration against the primary standard water calorimeter in this work.

	18 MeV		22 MeV	
Chamber	$N_{D,w}$ (cGy/nC)	k_Q	$N_{D,w}$ (cGy/nC)	k_Q
2006				
NE2571 #1	4.040(14)	0.907(3)	3.998(15)	0.898(3)
Scanditronix NACP-02	15.839(56)	0.895(3)	15.653(58)	0.885(3)
PTW Roos	7.647(27)	0.898(3)	7.571(28)	0.889(3)
2016				
NE2571 #1	4.039(14)	0.907(3)	4.006(15)	0.899(3)
NE2571 #2	4.084(14)	0.906(3)	4.052(15)	0.899(3)
PTW30013	4.857(17)	0.902(3)	4.815(18)	0.895(3)

component from the absorbed dose standard with 0.37 % from the combined uncertainty in table 1 we obtain an overall uncertainty of 0.41 % in $N_{D,w}$ coefficients derived through indirect calibration.

Table 3 also provides the difference between k_Q factors when more than one chamber of each type is used for measurements. Five NE2571 chambers are used for measurements and the difference between measurements in table 3 is the worst case difference between individual NE2571 chambers and the one calibrated directly against the calorimeter in 2006 and 2016. However, for other NE2571 chambers the difference is less than 0.1 %.

III.E. Long-term stability of ion chambers

Overall, the long-term stability of cylindrical chambers observed in this work is observed to be better than that for plane-parallel chambers. Differences in these ratios are typically less than 0.1 % over five years. In the worst case, the difference was 0.15 % for an Exradin A19 chamber. For plane-parallel chambers, even for NRC reference chambers (PTW Roos and Scanditronix NACP-02 chambers) differences are up to 0.3 % although they are typically better than 0.1 %. For other plane-parallel chambers, differences are typically at the 0.2-0.4 % level.

Table 3: Beam quality conversion factors for the 18 MeV beam obtained through indirect calibration of chambers against secondary standard reference chambers. The third column presents the maximum chamber-to-chamber variation for chambers of the same type where available.

Chamber type	k_Q	Maximum variation (%)
Plane-parallel		
PTW Roos	0.897	0.17
PTW Markus	0.896	0.11
PTW Advanced Markus	0.896	0.34
Scanditronix NACP-02	0.892	0.21
IBA PPC-05	0.895	0.11
IBA PPC-40	0.891	0.26
Exradin A10	0.923	
Exradin A11	0.920	
Cylindrical		
NE2571	0.907	0.27
IBA FC65-G	0.907	0.11
PTW 30013	0.902	0.08
Exradin A19	0.912	
Exradin A18	0.915	
Exradin A1SL	0.916	

IV. Discussion

IV.A. Comparison to other results

There are only a few publications that report k_Q factors for chambers in electron beams. The reference dosimetry protocols TG-51 and TRS-398 relied on a semianalytic approach to obtain k_Q factors (see section I.A.). Using Monte Carlo calculations of P_{wall} correction factors in Co with EGSnrc (rather than the less accurate EGS4 code system used for calculations for TG-51), Mainegra-Hing *et al.*[27] provide updated k_{ecal} factors for several plane-parallel chambers. Renaud *et al.*[12] used water calorimetry measurements to determine $k'_{R_{50}}$ values for PTW Roos and Exradin A12 chambers but they only provide k_{ecal} for the Exradin A12 chamber. Stucki and Vörös[28] provide k_Q factors for PTW Roos and NACP-02 chambers using Fricke ferrous sulphate dosimetry. Zink and Wulff[29] used Monte Carlo calculations to determine k_Q factors for four plane-parallel ion chamber types (PTW Roos, PTW Markus, PTW Advanced Markus and IBA NACP-02). Muir and Rogers[30] used similar Monte Carlo calculations to provide k_Q factors for several plane-parallel and cylindrical ion chamber types

and there is substantial overlap with the chambers investigated here. A comparison among results from different studies is difficult because of the various approaches used to define the point of measurement and the differences in beam qualities for the beams investigated in each publication.

IV.A.1. Comparison to measured results

The value of k_{ecal} (k_Q for a beam with R_{50}=7.5 cm, calculated from a fit to measured k_Q factors as a function of R_{50}) reported by Renaud *et al.*[12] for the Exradin A12 chamber is 0.903±0.004 and can be compared to the result obtained here for the Exradin A19 chamber, which has very similar specifications. They positioned the chamber at the reference depth but with a shift of $0.5 \times r_{\text{cav}}$ upstream of the point of measurement. A comparison is difficult because here we determine k_Q for the Exradin A19 with the chamber center at the reference depth only in the 18 MeV beam (R_{50}=7.05 cm). To compare, we account for the difference in shift using the gradient correction P_{gr} determined from depth-dose data in 18 MeV. We then use the difference in k_Q factors in 18 MeV and 22 MeV for those chambers that are calibrated directly against the primary calorimeter to determine the value of k_{ecal} for a beam with R_{50}=7.5 cm. This k_{ecal} factor amounts to 0.904, in very good agreement with the measured value of Renaud *et al.* although there will be a slightly higher uncertainty in this comparison value given the steps required to adjust these k_Q factors and using a value for the A19 compared to that for the A12.

Our results can also be compared to those of Stucki and Vörös[28] who calibrated PTW Roos and NACP-02 ion chambers against a Fricke ferrous sulphate dosimetry system. The differences for the PTW Roos (NACP-02) chamber are 0.5 % and 0.1 % (0.3 % and 1.0 %) in the 18 MeV and 22 MeV beams, respectively. These differences are slightly larger than one would hope when comparing results from two primary standards labs although they are still within combined uncertainties of about 1 % (k=1). However, Stucki and Vörös report chamber-to-chamber variations of 1.2 % and 1.9 % for PTW Roos and NACP-02 chambers, respectively, which could explain the source of the discrepency. We have not observed this type of variation in electron beams (see table 3) or photon beams.[31,32] In addition, the electron beam data reported by NPL is not subject to such variability.[33]

IV.A.2. Comparison to TG-51 protocol values

As with comparison to the measurement of Renaud *et al.*, one must adjust the k_Q factors measured here for comparison to TG-51 protocol k_{ecal} values. For the cylindrical chambers that are directly calibrated against the primary standard calorimeter the values are adjusted by applying the gradient correction in both the 18 MeV and 22 MeV beams and then interpolating as a function of R_{50} to get the value of k_{ecal} with R_{50}=7.5 cm. For chambers for which values of k_Q are only available in the 18 MeV beam through indirect calibration against reference chambers the same method of adjustment is used as for the A19 chamber for comparison to Renaud *et al.* above. For plane-parallel chambers, we use a water-equivalent scaling of the chambers' front face to position chambers at the point of measurement whereas TG-51 values are for plane-parallel chambers positioned with the inside of their front face at the reference depth. As noted in the Monte Carlo study by Muir and Rogers[30] and the TRS-398 protocol[3], this small difference in positioning makes little impact on k_Q or k_{ecal} factors for high-energy electron beams so no adjustment is made for this difference in point of measurement for comparison of results. To obtain the k_{ecal} factor for plane-parallel chambers calibrated directly against the primary standard calorimeter interpolation of the results in the 18 MeV and 22 MeV beam is used to get the value of k_{ecal} with R_{50}=7.5 cm. For chambers that are indirectly calibrated in the 18 MeV beam we adjust the value of k_Q using the difference in k_Q factors in 18 MeV and 22 MeV beams for the directly calibrated plane-parallel chambers. Table 4 compares the results measured here and adjusted for comparison to those provided in the TG-51 protocol. Differences are typically less than 0.5 % but are up to 1.3 % for the PTW Markus chamber.

Table 4 also compares these adjusted results to those from Mainegra-Hing *et al.*[27] who updated TG-51 k_{ecal} factors using Monte Carlo calculations of P_{wall} in a ^{60}Co beam with the EGSnrc code system. It was thought that these P_{wall} corrections were one of the main sources of error for TG-51 calculations of k_{ecal} because of potentially high systematic uncertainties associated with the use of the EGS4 code system.[34] The results of this work are in better agreement with those of Mainegra-Hing *et al.*[27] than TG-51 calculations for chambers that are available for comparison. However, for the Scanditronix NACP-02 the difference between these values and those of Mainegra-Hing *et al.* is 0.8 % and for the Exradin A10 the difference is 1.7 %. The updated calculations of Mainegra-Hing *et al.* still rely on the assumption that

Table 4: Comparison of the adjusted results of this work to those provided in the TG-51 protocol and the updated k_{ecal} factors of Mainegra-Hing *et al.*[27] Interpolation as a function of R_{50} is used to get the value of k_{ecal} for R_{50}=7.5 cm.

	k_{ecal}				
Chamber type	This work*	TG-51	Difference (%)	Mainegra-Hing *et al.*	Difference (%)
Plane-parallel					
Scanditronix NACP-02	0.892			0.885	0.82
PTW Roos	0.895	0.901	-0.62	0.896	-0.06
PTW Markus	0.893	0.905	-1.31	0.899	-0.63
PTW Advanced Markus	0.894			0.896	-0.25
Exradin A10	0.923			0.939	-1.73
Cylindrical					
NE2571	0.899	0.903	-0.40		
PTW30013[a]	0.895	0.897	-0.19		
Exradin A19[b]	0.904	0.906	-0.17		
Exradin A1SL[c]	0.911	0.915	-0.43		

* The values from this work are adjusted for comparison described in the text.
[a] TG-51 provides values for the PTW30001 chamber.
[b] TG-51 provides values for the Exradin A12 chamber.
[c] TG-51 provides values for the Exradin A1 chamber.

the wall correction factor in electron beams is unity and Buckley and Rogers[35] showed that this correction for the NACP-02 chamber in a beam with R_{50}=7.5 cm is 1.009, which would explain the difference between this work and that of Mainegra-Hing *et al.*

IV.A.3. Comparison to Monte Carlo calculations

Two recent publications provide Monte Carlo calculated k_Q factors in electron beams using the same method and the same Monte Carlo code system.[29,30] Muir and Rogers[30] compared their calculated values to those of Zink and Wulff[29] and found very good agreement. Therefore, we only compare the measured results obtained here to the more extensive set of calculations of Muir and Rogers. The comparison is only for values in the 18 MeV beam. No adjustment of the k_Q factors is required for cylindrical chambers since Muir and Rogers used the same point of measurement (the center of the chamber at the reference depth). Slightly different shifts of the point of measurement are used for plane-parallel chambers. Muir and Rogers used an optimal shift of the chambers' point of measurement that resulted in more

accurate determination of R_{50} from ion chamber calculations as a function of depth. For most chambers, this is very close to the shift determined through water-equivalent scaling of the chambers' front window, used for positioning plane-parallel chambers in this work. In addition, Muir and Rogers pointed out that small differences in positioning chambers in high-energy beams does not result in significant differences in k_Q factors. Therefore, no adjustment is made for different positioning of plane-parallel chambers to compare the two sets of data.

Table 5 shows the results of this comparison. Overall, the results for cylindrical chambers are in better agreement than for plane-parallel chambers with differences typically at the 0.1-0.2 % level and a maximum difference of 0.44 % for the Exradin A19 chamber. A larger difference between Monte Carlo calculations and measurements in MV photon beams was also observed for chambers that use C552 walls and, although steps were taken in an attempt to determine the source of this discrepancy, the issue remains unresolved.[15] For plane-parallel chambers, the results are up to 1.38 % different for the Exradin A11 chamber, outside of combined systematic uncertainties. This difference is interesting but likely not that important practically since these chambers are not widely used for electron beam dosimetry. What is perhaps more surprising is that the difference is much larger for the IBA PPC-40 than the PTW Roos even though the two chambers have almost identical specifications. We also observed larger differences for the PPC-40 chamber than the PTW Roos in MV photon beams[32] suggesting that there may be a real difference in terms of measurement performance for the two chambers. The chamber-to-chamber variability observed by Stucki and Vörös[28] could explain some of the larger differences in table 5 although other experimental data suggests that this may not be an issue.[32,33] In addition, varying the geometric dimensions of the ion chamber model used for Monte Carlo simulations of k_Q factors does not generate this type of variability.[36] Fortunately, for five of the eight plane-parallel chambers for which there is overlap between these two studies the differences are less than 0.5 %.

V. Conclusions

This work provides some of the best measurements of electron beam quality conversion factors by directly calibrating NRC secondary standard reference ion chambers against the NRC primary standard calorimeter in high-energy electron beams. We also provide k_Q

Table 5: Comparison of the measured results of this work to the Monte Carlo calculations of Muir and Rogers[30] in the 18 MeV beam (R_{50}=7.2 cm).

	k_Q		
Chamber type	This work	Muir and Rogers	Difference (%)
Plane-parallel			
PTW Roos	0.897	0.900	-0.28
PTW Markus	0.896	0.900	-0.46
PTW Advanced Markus	0.896	0.902	-0.68
Exradin A10	0.923	0.923	0.01
Exradin A11	0.920	0.907	1.38
Scanditronix NACP-02	0.892	0.894	-0.27
IBA PPC-05	0.895	0.894	0.07
IBA PPC-40	0.891	0.901	-1.20
Cylindrical			
NE2571	0.907	0.905	0.26
IBA FC65-G	0.907	0.905	0.17
PTW30013	0.902	0.903	-0.09
Exradin A19	0.912	0.908	0.44
Exradin A18	0.915	0.915	-0.05
Exradin A1SL	0.916	0.915	0.10

factors for several other ion chambers through indirect calibration against the secondary standard reference chambers in an 18 MeV beam. The additional uncertainty in deriving these k_Q factors through indirect calibration is small.

We compare these results to other publications that provide electron beam quality conversion factors. Differences ranged from 0.1 % to 1.0 % compared with other measurements, within combined uncertainties. Comparing to TG-51 protocol values and Monte Carlo calculations, differences are up to 1.7 % but are typically less than 0.5 %. These results will be useful for updated reference dosimetry protocols and this work represents a step toward the dissemination by NRC of electron beam quality conversion factors and ion chamber calibration coefficients for users.

VI. Acknowledgments

The authors thank Peter Brown of Mevex Corporation, Frantisek Gabris of IBA, Mark Szczepanski of PTW and Eric DeWerd of Standard Imaging for supplying the ion chambers

545 used for this work. The authors thank David Marchington and Mike Vandenhoff of the NRC
546 for the highly-skilled fabrication of the calorimeter vessels used in this work.

References

[1] P. R. Almond, P. J. Biggs, B. M. Coursey, W. F. Hanson, M. S. Huq, R. Nath, and D. W. O. Rogers, AAPM's TG–51 protocol for clinical reference dosimetry of high-energy photon and electron beams, Med. Phys. **26**, 1847 – 1870 (1999).

[2] M. R. McEwen, L. A. DeWerd, G. S. Ibbott, D. S. Followill, D. W. O. Rogers, S. M. Seltzer, and J. P. Seuntjens, Addendum to the AAPM's TG–51 protocol for clinical reference dosimetry of high-energy photon beams, Med. Phys. **41**, 041501(20pp) (2014).

[3] IAEA, Absorbed Dose Determination in External Beam Radiotherapy: An International Code of Practice for Dosimetry Based on Standards of Absorbed Dose to Water V12, Technical Report Series 398, `http://www-naweb.iaea.org/nahu/DMRP/documents/CoP_V12_2006-06-05.pdf`, 2006.

[4] A. R. DuSautoy, NPL calorimetry: The evolution so far, in *Proc. NPL Workshop on Recent Advances in Calorimetric Absorbed Dose Standards*, 2000.

[5] J. Seuntjens and S. Duane, Photon absorbed dose standards, Metrologia **46**, S39–S58 (2009).

[6] M. R. McEwen, Primary standards of air kerma for ^{60}Co and x rays and absorbed dose in photon and electron beams, in *Clinical Dosimetry Measurements in Radiotherapy*, edited by D. W. O. Rogers and J. E. Cygler, pages 501 – 547, Medical Physics Publishing, Madison, Wisconsin, 2009.

[7] T. Sander, S. Duane, N. Lee, C. Thomas, P. Owen, M. Bailey, and H. Palmans, NPL's new absorbed dose standard for the calibration of HDR ^{192}Ir brachytherapy sources, Metrologia **49**, S184 (2012).

[8] A. Guerra, S. Loreti, M. Pimpinella, M. Quini, M. D'Arienzo, I. Astefanoaei, C. Caporali, C. Bolzan, and M. Pagliari, A standard graphite calorimeter for dosimetry in brachytherapy with high dose rate ^{192}Ir sources, Metrologia **49**, S179 (2012).

575 [9] L. de Prez and J. de Pooter, The new NMi orthovolt x-rays absorbed dose to water
576 primary standard based on water calorimetry, Phys. Med. Biol. **53**, 3531 (2008).

577 [10] A. Krauss, L. Büermann, H.-M. Kramer, and H.-J. Selbach, Calorimetric deter-
578 mination of the absorbed dose to water for medium-energy x-rays with generating
579 voltages from 70 to 280 kV, Phys. Med. Biol. **57**, 6245 – 6268 (2012).

580 [11] M. R. McEwen and A. R. DuSautoy, Primary standards of absorbed dose for electron
581 beams, Metrologia **46**, S59–S79 (2009).

582 [12] J. Renaud, A. Sarfehnia, K. Marchant, M. McEwen, C. Ross, and J. Seuntjens, Di-
583 rect measurement of electron beam quality conversion factors using water calorime-
584 try, Med Phys **42**, 6357 (2015).

585 [13] M. R. McEwen and C. K. Ross, Direct calibration of ion chambers in linac electron
586 beams , Proceed. of Absorbed Dose and Air Kerma Primary Standards Workshop,
587 LNHB, Paris , http://www.nucleide.org/ADAKPS_WS/ (May, 2007).

588 [14] C. Hammond, CRC Handbook of Chemistry and Physics, 2015–2016, 2016.

589 [15] B. R. Muir, M. R. McEwen, and D. W. O. Rogers, Measured and Monte Carlo
590 calculated k_Q factors: accuracy and comparison, Med. Phys. **38**, 4600 – 4609 (2011).

591 [16] G. Bass, R. Thomas, and J. Pearce, The calibration of parallel-plate electron
592 ionization chambers at NPL for use with the IPEM 2003 code of practice: summary
593 data, Phys. Med. Biol. **54**, N115 – N124 (2009).

594 [17] J. P. Seuntjens, C. K. Ross, N. V. Klassen, and K. R. Shortt, A status report on the
595 NRC sealed water calorimeter, Technical Report PIRS–584, NRC Canada, Ottawa,
596 K1A 0R6, 1999.

597 [18] J. Medin, C. K. Ross, G. Stucki, N. V. Klassen, and J. P. Seuntjens, Commissioning
598 of an NRC-type sealed water calorimeter at METAS using ^{60}Co γ-rays, Phys. Med.
599 Biol. **49**, 4073 – 4086 (2004).

600 [19] R. J. Schulz and M. S. Weinhous, Convection currents in a water calorimeter, Phys.
601 Med. Biol. **30**, 1093–9 (1985).

602 [20] N. V. Klassen and C. K. Ross, Water calorimetry: the heat defect, Journal of
603 Research of the National Institute of Standards and Technology **102**, 63 (1997).

604 [21] A. Krauss, The PTB water calorimeter for the absolute determination of absorbed
605 dose to water in ^{60}Co radiation, Metrologia **43**, 259 (2006).

606 [22] C. Cojocaru, B. Muir, M. McEwen, C. Ross, N. Klassen, and D. Marchington, Sci-
607 Sat AM: Radiation Dosimetry and Practical Therapy Solutions-09: Stability of a
608 water calorimetry system as a primary standard for absorbed dose to water, Medical
609 Physics **43**, 4960–4961 (2016).

610 [23] C. K. Ross, J. P. Seuntjens, N. V. Klassen, and K. R. Shortt, The NRC Sealed
611 Water Calorimeter: Correction Factors and Performance, in *Proceedings of NPL*
612 *Workshop on Recent Advances in Calorimetric Absorbed Dose Standards*, edited
613 by A. J. Williams and K. E. Rosser, pages 90–102, National Physical Laboratory,
614 Teddington, UK, 2000.

615 [24] S. Picard, D. T. Burns, P. Roger, P. J. Allisy-Roberts, M. R. McEwen, C. D. Cojo-
616 caru, and C. K. Ross, Comparison of the standards for absorbed dose to water of
617 the NRC and BIPM for accelerator photon beams, Metrologia **47**, 06025 (2010).

618 [25] Joint Committee for Guides in Metrology (JCGM), Guide to the Expression of
619 Uncertainty in Measurement, JCGM 100:2008, 2008.

620 [26] B. R. Muir, M. R. McEwen, and D. W. O. Rogers, Determination of relative ion
621 chamber calibrations coefficients from depth-ionization measurements in clinical elec-
622 tron beams, Phys. Med. Biol. **59**, 5953 – 5969 (2014).

623 [27] E. Mainegra-Hing, I. Kawrakow, and D. W. O. Rogers, Calculations for plane-
624 parallel ion chambers in ^{60}Co beams using the EGSnrc Monte Carlo code, Med.
625 Phys. **30**, 179 – 189 (2003).

626 [28] G. Stucki and S. Vörös, Experimental $k_{Q,Q0}$ Electron Beam Quality Correction
627 Factors for the Types NACP02 and PTW34001 Plane-parallel Chambers, *Proceed.*
628 *of Absorbed Dose and Air Kerma Primary Standards Workshop*, LNHB, Paris ,
629 http://www.nucleide.org/ADAKPS_WS/ (May, 2007).

[29] K. Zink and J. Wulff, Beam quality corrections for parallel-plate ion chambers in electron reference dosimetry, Phys. Med. Biol. **57**, 1831–1854 (2012).

[30] B. R. Muir and D. W. O. Rogers, Monte Carlo calculations of electron beam quality conversion factors for several ion chamber types, Med. Phys. **41**, 111701 (15pp) (2014).

[31] M. R. McEwen, Measurement of ionization chamber absorbed dose k_Q factors in megavoltage photon beams, Med. Phys. **37**, 2179 – 2193 (2010).

[32] B. R. Muir, M. R. McEwen, and D. W. O. Rogers, Beam quality conversion factors for parallel-plate ionization chambers in MV photon beams, Med. Phys. **39**, 1618 – 1631 (2012).

[33] M. R. McEwen, S. Duane, and R. A. S. Thomas, Absorbed dose calibration factors for parallel-plate chambers in high energy photon beams, in *Standards and Codes of Practice in Medical Radiation Dosimetry; Proc. Int'l Symp, Vienna 25 – 28 Nov 2002*, volume 1, pages 335 – 341, IAEA, Vienna, 2003.

[34] D. W. O. Rogers, The physics of the AAPM's TG-51 protocol, in *Clinical Dosimetry Measurements in Radiotherapy*, edited by D. W. O. Rogers and J. E. Cygler, pages 239 – 296, Medical Physics Publishing, Madison, Wisconsin, 2009.

[35] L. A. Buckley and D. W. O. Rogers, Wall correction factors, P_{wall}, for parallel-plate ionization chambers, Med. Phys. **33**, 1788 – 1796 (2006).

[36] B. R. Muir and D. W. O. Rogers, Monte Carlo calculations for reference dosimetry of electron beams with the PTW Roos and NE2571 ion chambers, Med. Phys. **40**, 121722 (16pp) (2013).